N81-14167

THERMAL STRESS RESPONSE OF GENERAL PURPOSE HEAT SOURCE (GPHS) AEROSHELL MATERIAL

I. M. Grinberg*, L. E. Hulbert*,
and R. G. Luce*

ABSTRACT

A thermal stress test was conducted to determine the ability of the GPHS aeroshell 3-D FWPF material to maintain physical integrity when exposed to a severe heat flux such as would occur from prompt reentry of GPHS modules. The test was performed in the Giant Planetary Facility at NASA's Ames Research Center. Good agreement was obtained between the theoretical and experimental results for both temperature and strain time histories. No physical damage was observed in the test specimen. These results provide initial corroboration both of the analysis techniques used and that the GPHS reentry member will survive the reentry thermal stress levels expected.

INTRODUCTION

The General Purpose Heat Source (GPHS) is a radioisotope-fueled heat source to be used to provide electric power for the International Solar Polar Mission (ISPM) - Radioisotope Thermoelectric Generator (RTG). Modular in design, the GPHS consists of a series of modules stacked in sufficient quantity to meet the converter power requirements. Each heat source module contains four 62.5 W (thermal) PuO_2 fuel pellets and is rectangular parallelepiped in shape, as shown in the Figure 1 schematic.

The generator is designed to break apart during reentry into the earth's atmosphere, either following end-of-life or from a launch abort, exposing the stacked heat source modules to the environment. In turn, the stacked modules will separate due to aerodynamic forces such that the individual heat source modules will reenter the earth's environment. Release of the fuel during reentry and at earth impact is prevented by a combination of metal post-impact shell, carbon-based impact shell, and 3-D fine weave pierced fabric (FWPF) carbon-carbon aeroshell, and specific design characteristics selected on the basis of tests and analyses.

An accurate prediction of the thermal stress response of the GPHS module aeroshell is an important aspect of the overall heat source design. Many factors must be accurately accounted for in the analysis of material response, including material properties, heat flux distribution, and design features. Unfortunately, there is no adequate criterion available to predict the thermal stress failure of 3-D carbon-carbon, and relatively little experience and data base have been developed for the thermal stress resistance of the FWPF C/C

---

* Battelle, Columbus Laboratories, Columbus, Ohio.

material in accident environments that could result from applications of the GPHS. Thus, a meaningful comparison of thermal stress predictions with experimental data cannot be made without the generation of new data for the specific material of interest.

To overcome this lack of experience, a thermal stress test was designed and conducted on 3-D FWPF C/C to determine the ability of the aeroshell material to maintain physical and mechanical integrity when exposed to a severe heat flux environment such as would occur from prompt (steep angle) reentry of GPHS modules. Thermal and thermal stress analyses were performed to design the test model, select instrumentation, and determine the required environmental test conditions. The thermal stress test was conducted in the Giant Planetary Facility (GPF) at NASA's Ames Research Center (ARC).

ENVIRONMENTAL CONDITIONS

Reentry Environment

Test conditions were selected based on duplicating the peak tensile stress and strain levels in the GPHS module aeroshell that would result from prompt reentry of the GPHS modules. Initial conditions for this trajectory are reentry angle -89.9 degrees at an altitude of 121.9 km (400 kft) with a corresponding velocity of 10.97 kmps (36 kfps). Breakup of the generator and separation of the heat source modules are assumed to occur at 61 km (200 kft), an altitude sufficiently high to provide the peak aeroheating that would occur on this trajectory.

Reentry heating and pressure histories, along with freestream Reynolds number and Mach number histories, are shown in Figure 2 as a function of altitude. The stagnation point heating rate has been normalized to a 2.54 cm (1 in.) radius hemisphere. Reentry parameters for broad face stable and side face stable hypersonic modes are shown in Figure 2. The maximum aeroheating rate expected for the heat source module for this trajectory is approximately 47.7 MW/m^2 (4200 Btu/ft^2-sec) for the side on stable reentry mode.

Test Facility Selection

The NASA Ames 70 MW Giant Planetary Facility (GPF) was selected for the thermal stress test because this facility can provide the desired heating rates and can readily accommodate the test model configuration and size anticipated.

The arc heater in the GPF is capable of operating at a maximum electrical power input of 70 MW. A mixture of hydrogen and helium or hydrogen and nitrogen is used as the test gas. The nozzle used has a circular cross-section geometry and an exit diameter of 6.99 cm (2-3/4 in.). Based on previous thermal stress test experience with this nozzle, a flat faced, right circular cylindrical geometry test specimen was designed, with maximum model dimensions not to exceed 4.128 cm (1-5/8 in.) diameter and 8.57 cm (3-3/8 in.) length. With this test model geometry and size, an electrical power input of approximately 25 to 30 MW is required to achieve a stagnation point heat transfer rate on the test

model corresponding to peak heating conditions for the GPHS module during prompt reentry (side on stable hypersonic mode).

THERMAL STRESS TEST MODEL DESIGN

The thermal stress test model design is shown in Figure 3. This design is based on analyses conducted to determine the heat transfer rate for selected test facility operating conditions and the thermal and thermal stress response of the material. The flat face cylinder-flare configuration is consistent with thermal stress test experience at NASA Ames, and the overall size of the test specimen can be easily accommodated within the GPF facility. The axisymmetric configuration provides for symmetric external and internal boundary conditions and facilitates the thermal and thermal stress analyses. The specific wall thickness, 0.51 cm (0.2 in.), was selected to yield peak tensile stress and strain levels on the inside flat face surface of the FWPF C/C identical to the peak values expected during prompt reentry of the heat source module for the side on stable mode.

The flat inner surface of the front face allows for the application of both a thermocouple and an extensometer for measuring the back face temperature and strain history of the specimen.

The cylindrical portion and the integral tapered skirt were machined from a single block of Avco FWPF C/C material with the Z-fiber direction parallel to the axis of symmetry as shown in Figure 3. From the nominal diameter of 4.128 cm (1-5/8 in.), a Teflon flare is used to increase the overall diameter of the model assembly to 7.62 cm (3 in.) in a total assembled length of 8.57 cm (3-3/8 in.). The size of the aft-cone flare was selected so that the instrumentation package could be fit into the model assembly. Teflon was used for the cone-flare section in order to electrically insulate the C/C test model from the model sting. Threaded phenolic pieces are used to join the Teflon flare section to the C/C test model and the model assembly to the steel sting. The phenolic also serves to electrically insulate the model assembly from the sting. A 1.27 cm (1/2-in.) diameter hole is provided through the phenolic pieces to house components of the strain measuring instrumentation and to serve as a passage for electrical instrumentation wires.

Figure 4 shows the major components of the thermal stress test model. Shown in Figure 4 is the FWPF flat-faced cylinder flare, the Teflon flare with the forward phenolic connector, and other components which are identified and discussed in the following paragraphs.

The extensometer and back face thermocouple instrumentation assemblies for the thermal stress test models were specially developed and built to fit in the test specimen. Figure 5 is a schematic of the instrumentation package which fits into the 1.27 cm diameter hole in the pheonlic threaded pieces previously shown in Figure 3.

The main support bar is approximately 1.27 cm diameter and 4.45 cm (1-3/4-in.) long. Holes were drilled into the main support bar to (1) attach the 0.32 cm (1/8-in.) diameter tungsten forks (center-line distance between forks is

0.64 cm [1/4 in.]), (2) accommodate the thermocouple spring and alumina tube (approximately 0.32 cm diameter hole), (3) run the thermocouple leads through the main support (0.16 cm [1/16-in.) diameter hole), and (4) run the strain gage leads through the main support bar (0.32 cm-diameter hole). An electrical terminal was fastened to the face of the main support bar using epoxy cement in order to make the strain gage connections. The main support assembly is held in position using a spring which maintains the forks and thermocouple in contact with the back face of the C/C model.

Flat spots were gound on the tungsten forks where the four strain gages (Micro-Measurement Company, Model No. WK-06-0628P-350) were bonded to the forks using BR-G10 high temperature (260 C [500 F]) cement. The strain gages were used to measure bending strains in the forks. The ends of the forks were ground to a point with a total included cone angle of 60 degrees.

A 30 gage Pt-Pt/10 percent Rh thermocouple was used to measure the back face temperature of the C/C specimen. The thermocouple bead was ground to maximize its surface contact area with the back face of the C/C model (see detail, Figure 5). The bead was left rounded where it contacts the alumina tube in order to maintain a small contact area at this material interface. This bead geometry is commonly used to increase measuring accuracy. The contact area between the thermocouple bead and the C/C model was estimated to be approximately 400 times greater than the contact area at the alumina oxide tube interface.

SUPPORTING DESIGN ANALYSES

Thermal and thermal stress analyses were performed to determine the response of the FWPF C/C material to ensure that reentry stress levels would be achieved in the test model at arc heater conditions within the GPF operating envelope.

Thermal Analyses

Thermal analyses were performed to predict transient temperature distributions through the 3-D C/C test specimen as a function of specimen dimensions and GPF test conditions. A two-dimensional, transient heat-transfer computer program used to perform the reentry thermal and ablation analyses were used to perform the thermal analyses.

Table I shows the GPF operating conditions used in determining the thermal response of the 3-D C/C test model, corresponding to peak heating associated with a prompt GPHS reentry. At this arc heater operating condition, the stagnation point cold wall heat flux to the thermal stress test model is approximately 51.9 MW/m^2 (4570 Btu/ft^2-sec).

The nodal temperature-time history obtained from the thermal analysis was used as input for the thermal stress analysis.

Thermal Stress Analysis

Development of an axisymmetric thermal stress model allowed the application of computer program DOASIS to calculate the thermal stresses and strains for the test model configuration. This program has been well tested both for elastic and elastic-plastic strains.

A finite element model was developed for the test specimen using the two-dimensional model generation capability of the INGEN program developed by LASL.[1] This finite element model is shown in Figure 6. Temperatures were obtained for input into the DOASIS program by interpolation from the temperatures previously calculated using the finite difference code.

Elastic and elastic-plastic stress analyses were conducted to determine the suitability of the test model geometry and wall thickness using available elastic-plastic material property data. These analyses were made at various time intervals by inputting the specimen temperature distribution into the DOASIS computer program and iterating to obtain the elastic-plastic stresses. Although this procedure does not account for the time-dependent temperature history, the analyses are believed to be sufficiently accurate to demonstrate the stress relief obtained when the C/C composite undergoes compressive plastic flow at the front face surface.

Table II shows the results of the DOASIS analyses at various specimen exposure times. The DOASIS-calculated peak reentry tensile stress calculated using elastic-plastic property data is 103.4 MN/m^2 (15 ksi). From Table II, it can be seen that this stress level is predicted to occur at approximately 1 sec into the test.

Deformations of the test specimen were also predicted as part of the thermal stress analyses. Radial deformations computed at the forward inner cavity surface are compared with the measured deformations later in this paper.

INSTRUMENTATION CALIBRATION AND TEST PROCEDURES

Instrumentation used to measure the back face strain was calibrated prior to the conduct of the thermal stress test in the Ames GPF. Also a thermal analysis was conducted to determine the error in the back face temperature due to contact resistance at the FWPF C/C-thermocouple interface. Results of these activities are summarized as follows.

The strain gage extensometer used to measure the C/C specimen strain was calibrated after the strain gages and lead wires were attached. The sensitivity of the strain gage beam system was found to be 4184 με/MV/volt excitation.

Effects of temperature on the extensometer transducer's electrical output were checked by exposing the transducer to various temperature levels using a constant temperature oven.

Thermal analyses were conducted to determine the potential error in the temperature measurement that could result from poor contact between the thermocouple bead and the back face of the C/C test model. Although positive contact between the thermocouple bead and the C/C test model back face was maintained using a spring, there existed a thermal contact resistance at this interface. Based on information available for the contact conductance between tungsten and graphite[2] and a contact pressure of approximately 2.1 MN/m^2 (300 psi) at the thermocouple-C/C interface (cold pretrial measurement), a room temperature contact conductance of approximately 5674 W/m^2K (1000 Btu/hr-ft^2-F) was predicted between the thermocouple bead and the C/C material. During the test, there is a decrease in this conductance due to stress relaxation of the spring.

Results of this thermal analysis are presented in Figure 7 for the nominal heating rate conditions. The indicated thermocouple temperature reading is presented as a function of the actual back face temperature and contact conductance. For a contact conductance of 5674 W/m^2K (1000 Btu/hr-ft^2-F), the maximum difference between the indicated and actual back face temperatures is estimated to be approximately 121 to 149 C (250 to 300 F) over the test duration. Also shown in Figure 7 are the corrections that should be made to the indicated thermocouple reading for lower (1418, 2837 W/m^2K) and higher (28372 W/m^2K) contact conductances. For the latter value, there is practically no difference between the indicated and actual back face C/C temperature.

The effect of mechanical injection loads on the extensometer was evaluated by installing the test model in the holder and operating the sting which inserts the test model into the gas stream. The model was installed with the tungsten forks of the extensometer oriented in a direction perpendicular to the traversing direction of the sting. Placing the forks in this orientation minimizes the deceleration loads on the forks in the direction in which the strain would be measured.

Calibration tests were performed prior to testing of the FWPF test sample in order to determine the heater operating conditions required to achieve the desired nominal heating rate. A calorimeter model was used to measure the stagnation point heating rate.

Prior to inserting the FWPF test model into the arc-heated gas, the calorimeter model was inserted to ensure that the arc heater was functioning properly and the nominal heating rate of approximately 51 MW/m^2 was achieved.

The test model was inserted into the gas stream for approximately 3 seconds. During insertion, the model was protected by a nylon sabot which covered the cylindrical nose portion of the test sample. The two piece sabot was held in place around the test specimen using fine wires. The wires usually melt in approximately 200 to 500 msec, depending on the arc heater operating conditions, and the sabot is forced away from the model by the high dynamic pressures associated with the gas stream. The elapsed time associated with the removal of the sabot after the retainer wires are melted is of the order of a millisecond. Thus, the test model is subjected to a step-like change in environment.

An optical pyrometer was used to measure the front face stagnation point temperature history.

TEST RESULTS

The oscillograph measurement of back face temperature and strain are shown in Figure 8 along with the predicted back face temperature and strain histories. A corrected back face temperature history is also shown in Figure 8 using the measured temperatures and a FWPF C/C-thermocouple contact conductance of 2837 W/m^2K.

It can be seen that there is good agreement between the predicted and measured temperature history (based on contact conductance of 2837 W/m^2K), and that the predicted strain levels are in good agreement with the measured values. The slopes of the predicted and measured strain histories are practically identical to each other with a difference in strain of approximately 200 μm/m. The predicted strain values are based on the back face temperature history using a contact conductance of 2837 W/m^2K.

No cracks or other physical damage was observed in the test specimen even though the tensile stresses and strains reached those levels expected during reentry of the GPHS module. This provides initial corroboration that the GPHS reentry member will survive reentry thermal stresses.

CONCLUSIONS

The thermal stress test conducted in the NASA Ames Giant Planetary Facility (GPF) demonstrated that the Avco FWPF C/C composite can withstand GPHS prompt reentry heat flux, stress, and strain levels without suffering noticeable damage or loss of physical integrity.

The predictive techniques used to calculate the thermal and thermal stress response of the FWPF C/C aeroshell material were found to be in good agreement with the measured values following appropriate corrections for contact resistance between the specimen back face and the thermocouple bead. Although this comparison is based only on one test, the agreement lends credence to the theoretical methods being used in predicting temperatures and strains of FWPF C/C.

It was demonstrated that the strain/deformation developed by FWPF C/C, when subjected to severe reentry environment heat flux levels, could be successfully measured through proper design and calibration of a newly-conceived instrumented system.

For further corroboration of the theoretical methods, as well as obtaining further proof of the durability of the C/C composite, additional FWPF C/C specimen tests are needed at various heat flux levels characteristic of GPHS prompt reentry conditions such that the failure stress/strain levels can be determined and associated with specific initial reentry trajectory conditions.

REFERENCES

(1) Cook, William A. "INGEN, A General Purpose Mesh Generator for Finite Element Codes", Los Alamos Information Report LA-7135-MS, March, 1978, 19 pp and appendices.

(2) Rohsenow, W. M., and Hartnett, J. P., "Handbook of Heat Transfer", McGraw-Hill Book Company, New York, 1973, Chapter 3.

TABLES

TABLE I. INPUT VALUES FOR THERMAL ANALYSIS OF THERMAL STRESS MODEL

Stagnation Values			Free-Stream Conditions		Cold Wall Stagnation Point Heating Rate to 2.54 cm Radius Hemisphere, MW/m^2
Enthalpy MJ/kg	Model Impact Pressure, N/m^2	GPHS Heating Rate (Cold Wall), MW/m^2	Mach Number	Velocity, m/sec	
81.4	1.5×10^5	51.9	1.7	2,591	79.2

TABLE II. ELASTIC AND ELASTIC-PLASTIC THERMAL STRESSES

Time, Sec	Maximum Tensile Stress, MN/m^2		Maximum Compressive Stress, MN/m^2	
	Elastic	Elastic-Plastic	Elastic	Elastic-Plastic
		Nominal Heating Rate		
0.25	69	55	-200	-145
0.51	97	76	-159	-124
0.75	110	90	-138	-124
0.94	117	103	-131	-117
1.28	117	117	-117	-117

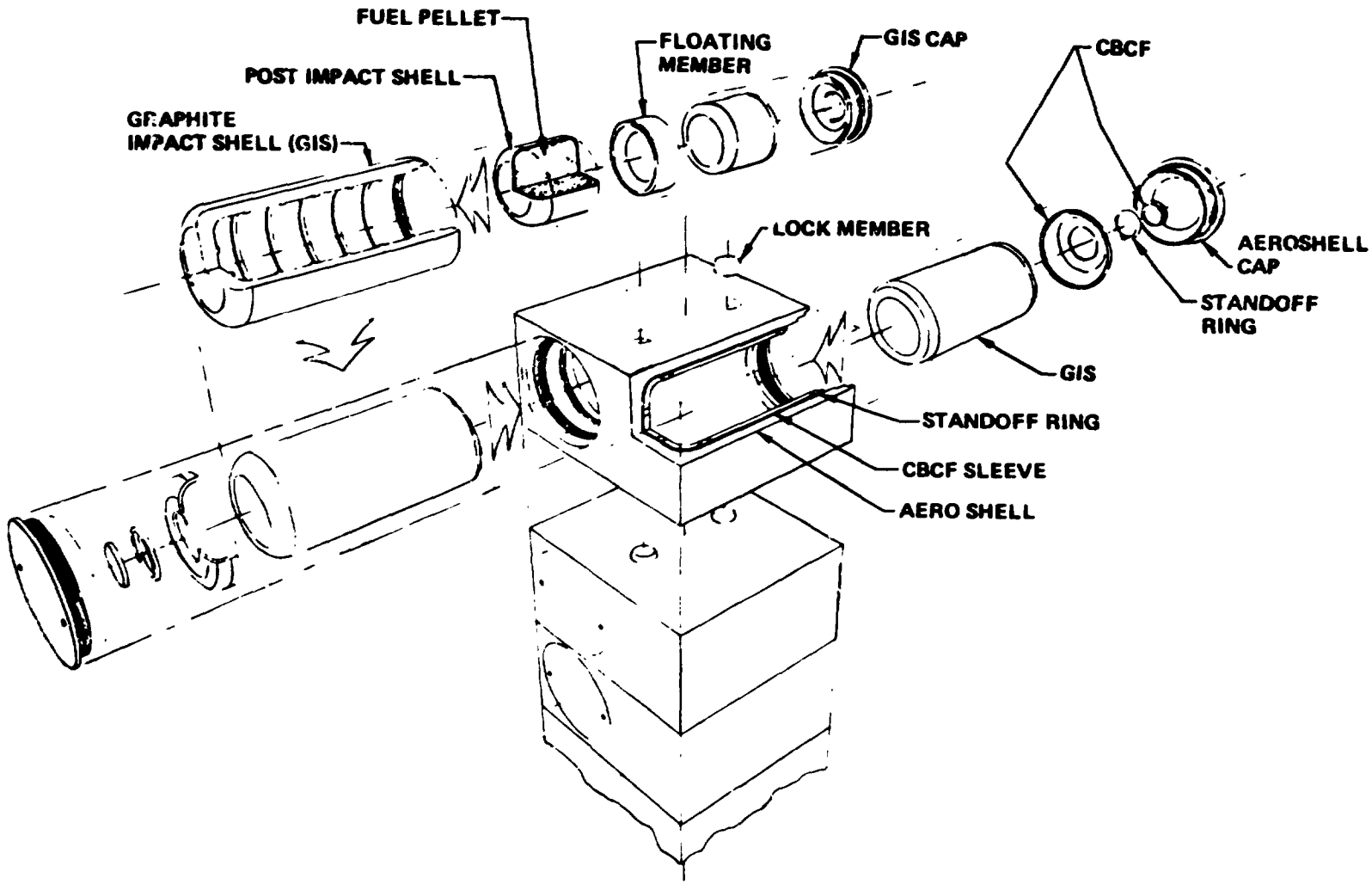

Figure 1. GPHS Module Schematic

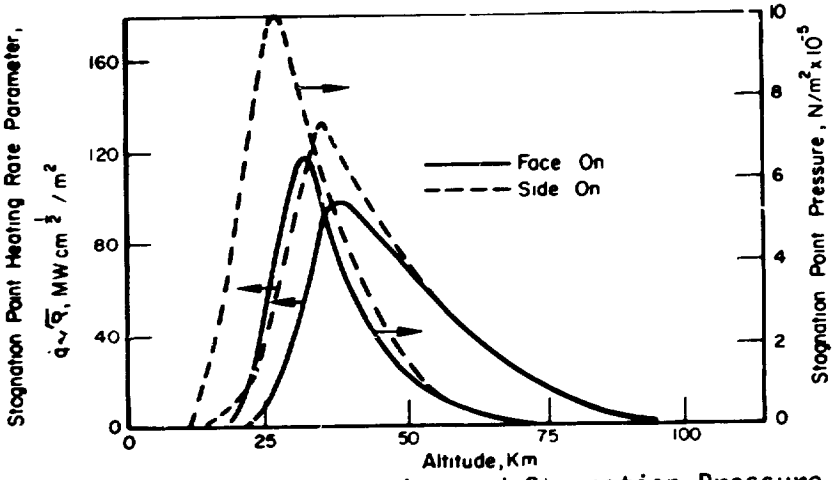

Figure 2a. Reentry Heating and Stagnation Pressure

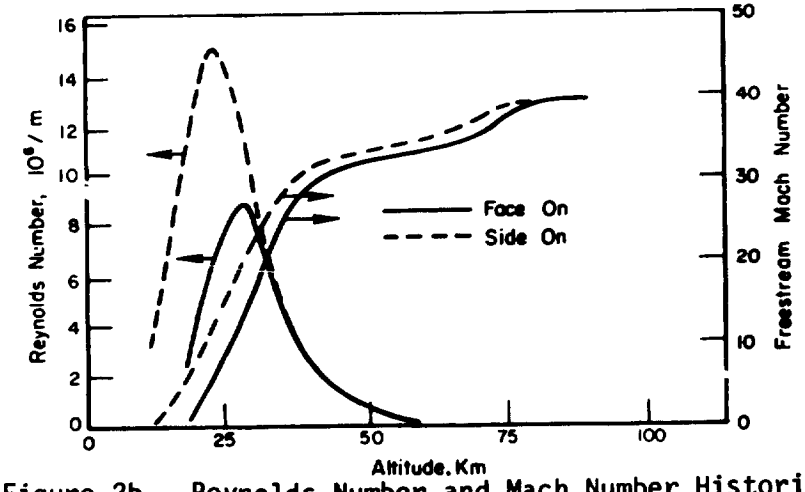

Figure 2b. Reynolds Number and Mach Number Histories

Figure 2. Prompt Angle Reentry Parameters

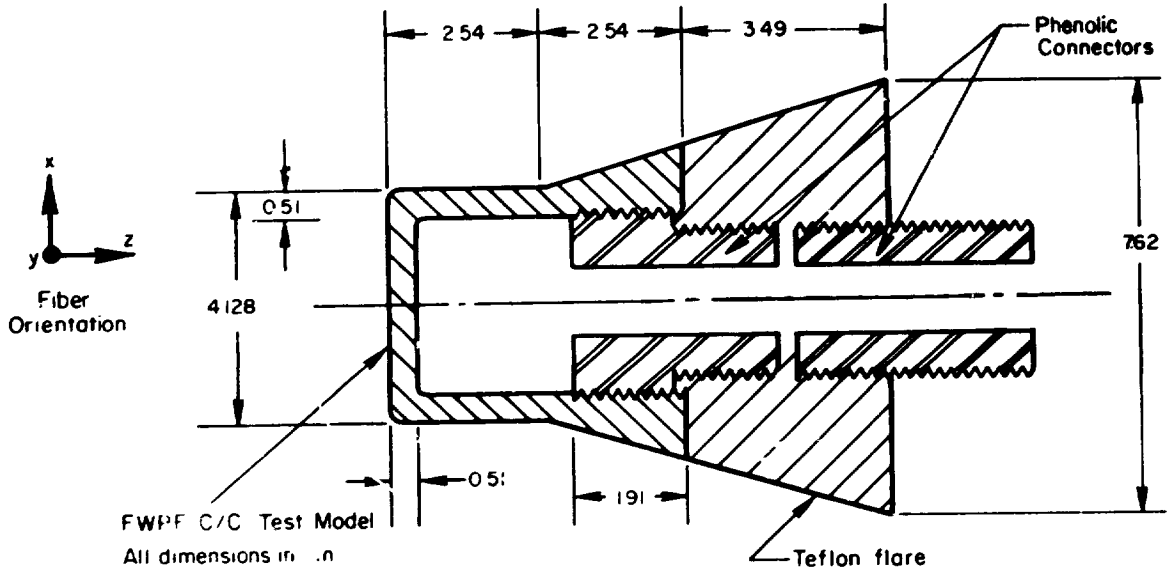

Figure 3. Cross-Sectional Drawing of Thermal Stress Model

Figure 4. Photograph of Thermal Stress Model Components

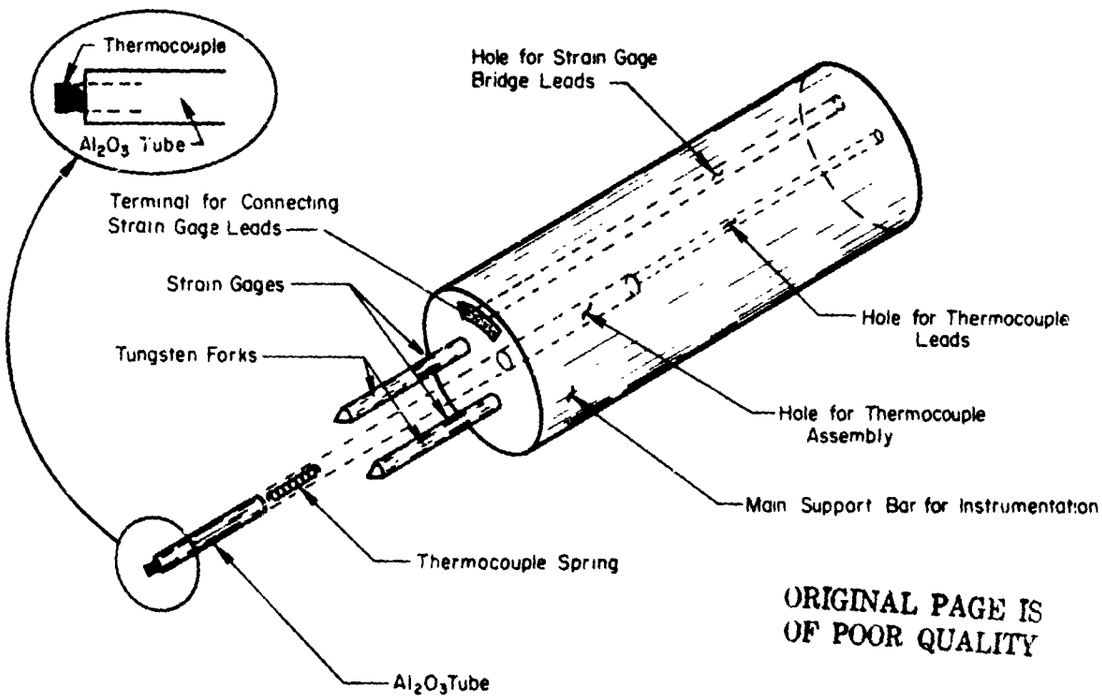

Figure 5. Schematic of Instrumentation Package for the Thermal Stress Tests

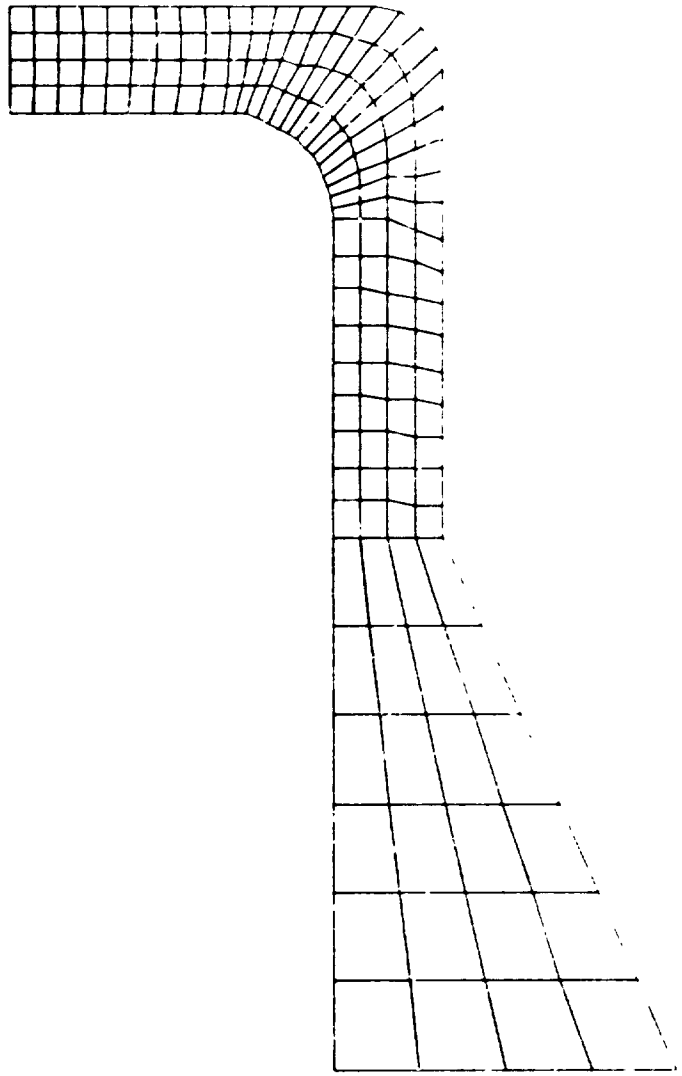

Figure 6. Finite Element Model of the Thermal Stress Test Model

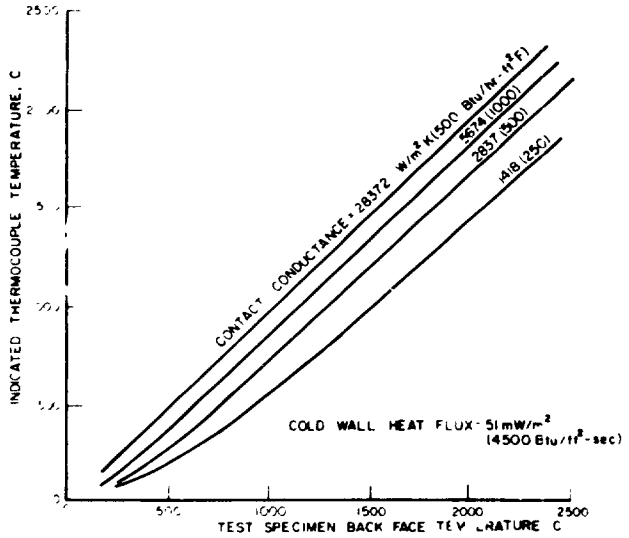

Figure 7. Back Face Thermocouple Response As a Function of Back Face Temperature and Contact Conductance

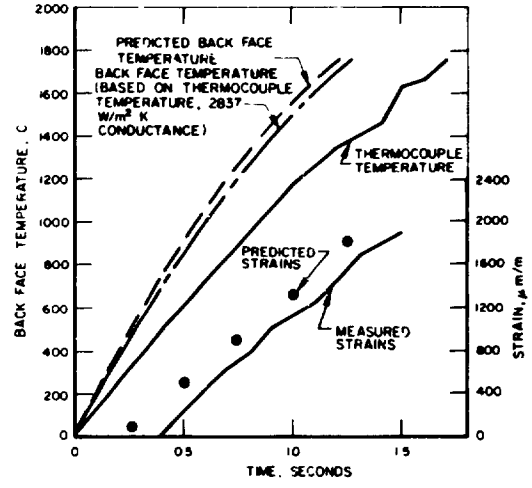

Figure 8. Thermal Stress Test, Comparison of Experiment and Analysis